CORA Cork Open Research Archive
Cartlann Taighde Oscailte Chorcaí

Title	Surprising evolution of the parsec-scale Faraday Rotation gradients in the jet of the BL Lac object B1803+784
Authors	Mahmud, Mehreen;Gabuzda, Denise;Bezrukovs, V.
Publication date	2009
Original Citation	Mahmud, M., Gabuzda, D. C. and Bezrukovs, V. (2009) 'Surprising evolution of the parsec-scale Faraday Rotation gradients in the jet of the BL Lac object B1803+784', Monthly Notices of the Royal Astronomical Society, 400(1), pp. 2-12. doi: 10.1111/j.1365-2966.2009.15013.x
Type of publication	Article (peer-reviewed)
Link to publisher's version	https://academic.oup.com/mnras/article-lookup/doi/10.1111/j.1365-2966.2009.15013.x - 10.1111/j.1365-2966.2009.15013.x
Rights	© 2009, the Authors. Journal compilation © 2009, RAS
Download date	2026-11-17 12:17:09
Item downloaded from	https://hdl.handle.net/10468/4968



UCC
University College Cork, Ireland
Coláiste na hOllscoile Corcaigh

Monthly Notices
of the
ROYAL ASTRONOMICAL SOCIETY

Mon. Not. R. Astron. Soc. **400,** 2–12 (2009) doi:10.1111/j.1365-2966.2009.15013.x

Surprising evolution of the parsec-scale Faraday Rotation gradients in the jet of the BL Lac object B1803+784

M. Mahmud,[1⋆] D. C. Gabuzda[1] and V. Bezrukovs[2]

[1]*Physics Department, University College Cork, Cork, Ireland*
[2]*Applied Physics and Instrumentation Department, Cork Institute of Technology, Cork, Ireland*

Accepted 2009 May 3. Received 2009 May 1; in original form 2008 August 8

ABSTRACT

Several multifrequency polarization studies have shown the presence of systematic Faraday Rotation gradients across the parsec-scale jets of active galactic nuclei, taken to be due to the systematic variation of the line-of-sight component of a helical magnetic (***B***) field across the jet. Other studies have confirmed the presence and sense of these gradients in several sources, thus providing evidence that these gradients persist over time and over large distances from the core. However, we find surprising new evidence for a reversal in the direction of the Faraday Rotation gradient across the jet of B1803+784, for which multifrequency polarization observations are available at four epochs. At our three epochs and the epoch of Zavala & Taylor, we observe transverse rotation measure (RM) gradients across the jet, consistent with the presence of a helical magnetic field wrapped around the jet. However, we also observe a 'flip' in the direction of the gradient between 2000 June and 2002 August. Although the origins of this phenomenon are not entirely clear, possibly explanations include (i) the sense of rotation of the central supermassive black hole and accretion disc has remained the same, but the dominant magnetic pole facing the Earth has changed from north to south, (ii) a change in the direction of the azimuthal ***B*** field component as a result of torsional oscillations of the jet and (iii) a change in the relative contributions to the observed RMs of the 'inner' and 'outer' helical fields in a magnetic-tower model. Although we cannot entirely rule out the possibility that the observed changes in the RM distribution are associated instead with changes in the thermal-electron distribution in the vicinity of the jet, we argue that this explanation is unlikely.

Key words: BL Lacertae objects: individual: B1803+784 – galaxies: jets – galaxies: magnetic fields.

1 INTRODUCTION

BL Lac objects are active galactic nuclei (AGN), characterized by strong and variable polarization, rapid variability in luminosity, a featureless spectrum and weak optical line emission. The radio emission associated with BL Lac objects is synchrotron emission, which can be linearly polarized up to about 75 per cent in the optically thin (jet) region, and up to 10–15 per cent in the optically thick (core) region (Pacholczyk 1970). Very long baseline interferometry (VLBI) polarization observations of BL Lac objects have shown a tendency for the polarization ***E*** vectors in the parsec-scale jets to be aligned with the local jet direction, which implies that the corresponding ***B*** field is transverse to the jet, because the jet is optically thin (Gabuzda, Pushkarev & Cawthorne 2000). Although in the past, the dominance of the transverse ***B*** field component was suggested to be the consequence of a 'shock model' where a series of relativistic shocks compress and enhance the transverse ***B*** field component (Laing 1980; Hughes, Aller & Aller 1989), this seems an improbable explanation for the transverse fields detected in extended regions in the jets of some sources. Instead, a helical ***B*** field associated with the jet, with the toroidal component dominating over the longitudinal component, would be a more plausible explanation (Lyutikov, Pariev & Gabuzda 2005). In fact, systematic gradients in the Faraday Rotation have been observed across the parsec-scale jets of a number of AGN, interpreted as reflecting the systematic change in the line-of-sight component of a toroidal or helical jet ***B*** field across the jet (Asada et al. 2002; Gabuzda, Murray & Cronin 2004; Zavala & Taylor 2005; Asada et al. 2008a,b; Gabuzda et al. 2008; Mahmud & Gabuzda 2008); such fields would come about in a natural way as a result of the 'winding up' of an initial 'seed' field by the rotation of the central accreting objects (e.g. Nakamura, Uchida & Hirose 2001; Lovelace et al. 2002).

Faraday Rotation studies are crucial in determining the intrinsic ***B*** field geometries associated with the jets. Faraday Rotation of the plane of linear polarization occurs during the passage of an electromagnetic wave through a region with free electrons and a magnetic field with a non-zero component along the line of sight.

⋆E-mail: mahmud@physics.ucc.ie

© 2009 The Authors. Journal compilation © 2009 RAS

The amount of rotation is proportional to the integral of the density of free electrons n_e multiplied by the line-of-sight $\boldsymbol{B}$ field $\boldsymbol{B} \cdot \mathrm{d}\boldsymbol{l}$, the square of the observing wavelength λ^2 and various physical constants; the coefficient of λ^2 is called the rotation measure (RM):

$$\Delta\chi \propto \lambda^2 \int n_e \boldsymbol{B} \cdot \mathrm{d}\boldsymbol{l} \equiv \mathrm{RM}\lambda^2. \quad (1)$$

The intrinsic polarization angle can be obtained from the following equation:

$$\chi_{\mathrm{obs}} = \chi_0 + \mathrm{RM}\lambda^2, \quad (2)$$

where χ_{obs} is the observed polarization angle and χ_0 is the intrinsic polarization angle observed if no rotation occurred (Burn 1966). Simultaneous multifrequency observations thus allow the determination of the RM, as well as identifying the intrinsic polarization angles χ_0.

B1803+784 has been studied using VLBI for nearly three decades. The predominant jet direction in centimetre-wavelength images is towards the west. The dominant jet $\boldsymbol{B}$ field is perpendicular to the local jet direction essentially throughout the jet, from distances of less than 1 mas from the VLBI core (Gabuzda 1999; Lister 2001) to tens of mas from the core (Gabuzda & Chernetskii 2003; Hallahan & Gabuzda 2009); further, the $\boldsymbol{B}$ field remains orthogonal even in extended regions and in the presence of appreciable bending of the jet. Therefore, it seems most likely that this transverse jet $\boldsymbol{B}$ field primarily represents the toroidal component of the intrinsic $\boldsymbol{B}$ field of the jet, rather than a series of transverse shocks (of course, this does not rule out the possibility that some individual compact features may be shocks). We have detected a transverse RM gradient across the VLBI jet; although it is difficult to prove conclusively, combined with the observation of orthogonal $\boldsymbol{B}$ fields throughout the jet, even in the presence of appreciable bending, this provides direct evidence that the jet has a helical $\boldsymbol{B}$ field. Comparison of the gradients observed for several different epochs shows that the direction of the gradient changed sometime between 2000 June and 2002 August. We discuss the data demonstrating this unexpected change, as well as possible origins of the observed reversal of the RM gradient.

2 FARADAY ROTATION OBSERVATIONS AND REDUCTION

We consider here polarization data for B1803+784 obtained using the ten 25-m radio telescopes of the Very Long Baseline Array (VLBA) at four different epochs: 1997 April 6 (Gabuzda & Chernetskii 2003), 2000 June 27 (Zavala & Taylor 2003), 2002 August 24 and 2003 August 22. Table 1 lists the observing frequencies for each epoch. The observations for 2002 August 24 and 2003 August 22 were obtained as part of a multifrequency polarization study of about three dozen BL Lac objects. In all cases, the sources were observed in a 'snapshot' mode with 8–10 scans of each object spread out over the time. The preliminary calibration, D-term calibration and polarization calibration were all done in AIPS using standard techniques. For more detailed calibration information for the 1997 data, see Gabuzda & Chernetskii (2003) and Reynolds, Cawthorne & Gabuzda (2001), and for the 2000 June data see Zavala & Taylor (2003).

Note that Gabuzda & Chernetskii (2003) presented results at 22 GHz in addition to the 15, 8.4 and 5 GHz results considered here; we did not include the 22 GHz data in our Faraday Rotation analysis because this substantially restricted the region in the jet where polarization was reliably detected at all the frequencies used. In regions where polarization was detected at 22, 15, 8.4 and 5 GHz, the derived RMs are consistent with the three-frequency results presented here.

Table 1. Observational parameters.

Epoch	Frequency (GHz)
1997 April 6	4.990, 8.415, 15.285, 22.221†
2000 June 11	8.114, 8.209, 8.369, 8.594, 12.115, 12.591, 15.165‡
2002 August 24	15.286, 22.234, 43.136
2003 August 22	4.612, 5.092, 7.916, 8.883, 12.939, 15.383

†Gabuzda & Chernetskii (2003).
‡Zavala & Taylor (2003).

2.1 2002 August 24 and 2003 August 22

The instrumental polarizations (D-terms) were determined using the AIPS task LPCAL, solving simultaneously for the source polarization in individual VLBI components. The sources used for this purpose were 1308+326 (2002 August) and 1156+295 (2003 August). The Electric Vector Polarization Angle (EVPA) calibration was done using integrated polarization observations of a bright, compact source, obtained with the Very Large Array (VLA), by forcing the EVPA for the total VLBI polarization of the source to match the EVPA for the integrated polarization (http://www.aoc.nrao.edu/∼smyers/calibration/). The sources used for the EVPA calibration were 1749+096 (observed with the VLA on 2002 August 10) and 2200+420 (observed with the VLA on 2002 August 18 and 2003 August 21). The sources were observed with the VLA at frequencies 5, 8.5, 22 and 43 GHz. We found the obtained values to be consistent with the (Faraday Rotation) linear λ^2 law and were thus able to interpolate from the graph the corresponding values for our non-standard frequencies. We refined the calibration by checking for self-consistency between the various frequencies, and also with the other EVPA calibration results for VLBA experiments before and after ours that were calibrated using the same reference antenna (the EVPA corrections for a given reference antenna are typically stable to within $\chi \sim 5^\circ$ over several years; see Reynolds et al. 2001, http://www.physics.purdue.edu/MOJAVE/allsources.html). Table 2 shows the final applied EVPA corrections.

The 2003 August data include several frequencies that differ from the standard 5, 8 and 15 GHz frequencies for the VLBA. Although system temperatures and gain curves were provided for all six frequencies observed at this epoch, there may be some concern that the accuracy of the overall flux calibration for these slightly

Table 2. Electric vector position angle (EVPA) corrections.

Epoch	Frequency (GHz)	Reference antenna	EVPA correction $\Delta\chi$ (°)
2002 August 24	15.2855	LA	+92
	22.2346	LA	+35
	43.1355	LA	+75
2003 August 22	4.6120	LA	−66
	5.0920	LA	−66
	7.9160	LA	+103
	8.8830	LA	+92
	12.9390	LA	+81
	15.3830	LA	+109

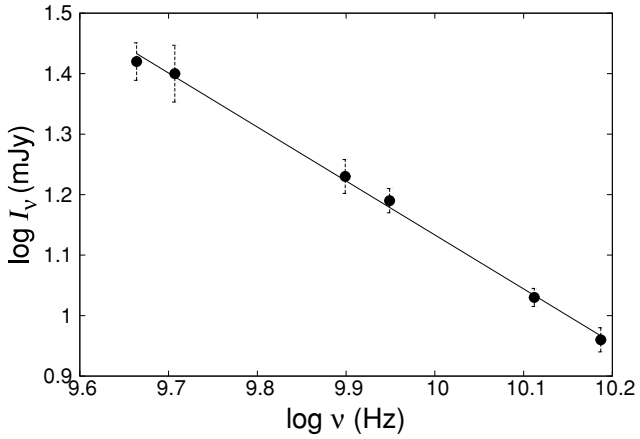


Figure 1. Plot of $\log I_\nu$ (mJy) versus $\log \nu$ (Hz) for a 3 × 3 pixel area in the optically thin jet of B1803+784. The observed spectrum is fully consistent with a power law, with spectral index -0.89 ± 0.02. There is no evidence for deviations from this behaviour for any of the six observing frequencies.

'non-standard' frequencies could be slightly lower than for the standard VLBA frequencies. Accordingly, we determined the spectra of various optically thin regions in the jet, to verify that there was no evidence for any of the frequencies deviating from the behaviour shown by the others. Before determining the spectra, we aligned the images at various frequencies using the algorithm of Croke & Gabuzda (2008). A typical example, corresponding to a position 3.4 mas west and 0.3 mas north of the VLBI core, is shown in Fig. 1; we can see that the observed 4.6–15.3 GHz fluxes are all consistent with a power law within the errors, corresponding to a 'normal' optically thin spectral index of -0.89 ± 0.02. Thus, we find no evidence for inaccuracy of the overall flux calibration at any of our six frequencies.

We made maps of the distribution of the total intensity I and Stokes parameters Q and U at the different frequencies with matched resolutions corresponding to the lowest- or middle-frequency beam. The distributions of the polarized flux ($p = \sqrt{Q^2 + U^2}$) and polarization angle ($\chi = \frac{1}{2} \arctan \frac{U}{Q}$) were obtained from the Q and U maps using the AIPS task COMB. We then constructed maps of the RM using a modified version of the AIPS task RM that can construct RM maps using up to 10 frequencies, obtained from R. Zavala (we will be happy to provide this code to anyone who is interested), after subtracting the effect of the integrated RM (presumed to arise in our Galaxy) from the observed polarization angles (the integrated RM value for B1803+784 was -60 rad m^{-2}, determined by Pushkarev 2001), so that any residual Faraday Rotation was due to only the thermal plasma in the vicinity of the AGN. The RMs and associated (χ) uncertainties were determined in a similar manner to that used by Gabuzda et al. (2004), taking into account the errors in the angle calibration (3°), as well as the error in the polarization angles [which were taken to be the rms deviation from the mean value of 3 × 3 pixel (0.3 × 0.3 mas^2) area at the corresponding location].

3 RESULTS

The total intensity (I), linear polarization (P) and RM maps for epoch 2000 June 11 are presented by Zavala & Taylor (2003), and I and P maps for 1997 April 6 by Gabuzda & Chernetskii (2003); we present the RM map for the latter epoch below. An angular distance of 1 mas corresponds to a linear distance of 7.06 pc at the redshift (0.68) of B1803+784 (http://www.physics.purdue.edu/MOJAVE/sourcepages/1803+784.shtml).

Figs 2 and 3 show the observed VLBI total intensity and linear polarization structures for 2002 August and 2003 August. The peaks and bottom contours of these maps are given in Table 3. The images in Figs 4–6 show the VLBI total intensity contours for 1997 April 6, 2002 August 24 and 2003 August 22 with their parsec-scale RM distributions superimposed. In all the maps presented here, the contours increase in steps of a factor of 2, and the beam is shown in the lower-left corner of the image.

The polarization maps for all four epochs are consistent with a predominantly transverse magnetic field structure. Transverse RM gradients are visible across the VLBI jet of B1803+784 in each of the three epochs shown in Figs 4–6, on scales of ∼2–3 mas; we are also tentatively able to follow the RM gradient further from the core in Fig. 6. This supports the hypothesis that this jet has a helical magnetic field, consistent with the observed transverse magnetic field structure. The arrows show the directions of the RM gradients in the corresponding regions; in other words, the direction in which the value of the RM increases (from more negative to less negative, negative to positive or less positive to more positive, as the case may be). The accompanying panels show plots of polarization angle (χ) versus wavelength squared (λ^2) for the indicated regions, as well as slices through the RM distributions between the indicated points. The uncertainties in the polarization angles are also shown in the plots.

Fig. 7 shows plots of the observed RM as a function of the transverse distance from the central spine of the jet. The errors in the RMs in these plots were estimated in the same way as for the χ values, by calculating the mean RM within the corresponding 3 × 3 pixel area in the map and assigning the rms deviation about this mean as the RM error. We consider this approach to be most reasonable, since possible EVPA calibration errors will affect the fitted RM values and the uncertainties derived from the fits, but not the inferred RM gradients, as is shown in Appendix A. Both these plots and the RM slices in Figs 4–6 clearly demonstrate the systematic, monotonic nature of the observed RM gradients.

The RM map of Zavala & Taylor (2003) for 2000 June also shows a clear transverse gradient, with a negative RM along the northern edge of the jet and less negative or positive RM along the southern edge, similar to the RM map observed in 2002 August (Fig. 5). An important feature that emerges in a comparison of various RM maps is the reversal in the direction of the RM gradient in the jet of B1803+784 between 2000 June and 2002 August. The RM values increase towards the southern edge of the jet in the 1997 April and 2000 June (Zavala & Taylor 2003) RM maps, but towards the northern edge of the jet in the 2002 August and 2003 August RM maps.

We also observe gradients in the core region for all three of our epochs, shown by the arrows in the core region in Figs 4–6, all of which are in the same direction (i.e. the 'flip' of the gradient occurred only in the jet region). There are hints of a RM gradient with the same direction in the core in the map presented by Zavala & Taylor (2003), but the range for the colour scale of that map makes it difficult to be sure of this. Note that the observed 'core' emission is actually a mixture of emission from the core and inner jet, so it is not surprising that transverse RM gradients should be detected in the core region, since the associated helical field is present on a wide range of scales, down to the accretion disc region.

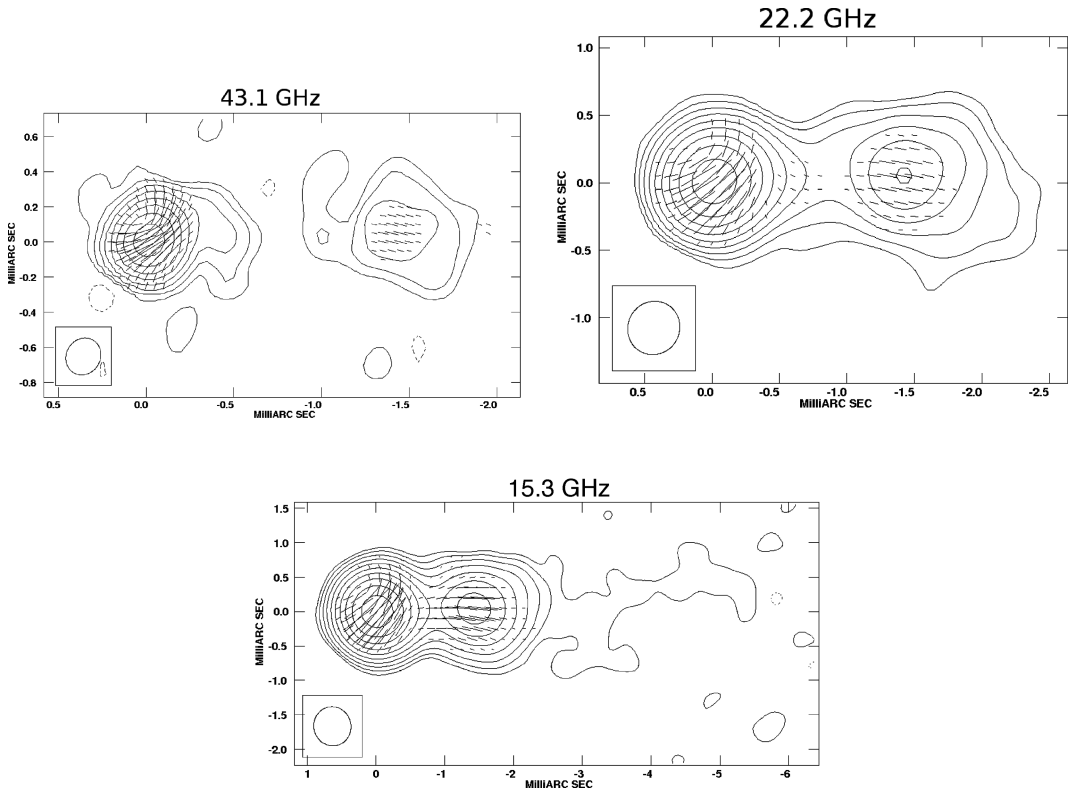


Figure 2. VLBA *I* maps with (electric vector) polarization sticks superimposed at 43.1, 22.2 and 15.3 GHz at epoch 2002 August 24, corrected for integrated Faraday Rotation.

4 DISCUSSION

4.1 Possible origins of the RM-gradient reversal

The origin of the observed 'flip' in the direction of the transverse RM gradient in the jet of B1803+784 between 2000 June and 2002 August is not clear. No radical change in the intensity or polarization structure of the VLBI jet accompanied the observed RM-gradient flip. We qualitatively consider here several possible scenarios that could potentially give rise to this behaviour. Although it is not possible at this stage to distinguish between these scenarios, our goal here is simply to point out possible explanations, which it may be possible to test with further observations or numerical simulations.

In this discussion, we will suppose that the RM gradient is associated with a helical jet $\boldsymbol{B}$ field that is due to the rotation of the central black hole. In this case, the direction of the observed transverse RM gradient is determined by the direction of rotation of the black hole and the 'polarity' of the poloidal field component, i.e. north or south/outwards or inwards relative to the black hole.

Reversal of the 'pole' of the black hole facing the Earth. It is obviously not reasonable to suppose that the observed reversal in the RM gradient is due to a change in the direction of rotation of the central black hole. However, one way to retain a transverse RM gradient in a helical magnetic field model, but reverse the direction of this gradient, is if the direction of rotation of the central black hole (i.e. the direction in which the field threading the accretion disc is 'wound up') remains constant, but the 'pole' of the black hole facing the Earth changes from north to south, or vice versa (Fig. 8). To our knowledge, it is currently not known whether such polarity reversals are possible for AGN jets, or whether they could occur on a time-scale as short as a few years. Numerical simulations of the generation and propagation of helical magnetic fields for various initial seed-field configurations could potentially answer these questions.

Torsional oscillations of the jet. Another way in which the direction of the azimuthal component of a helical $\boldsymbol{B}$ field could change is as a result of torsional oscillations of the jet, such as those that have been proposed by Bisnovatyi-Kogan (2007). These torsional oscillations, which may stabilize the jets, essentially correspond to a change in the direction of rotation of the jet, and could cause reversals of the azimuthal $\boldsymbol{B}$ field component from time to time, probably periodically or quasi-periodically. Of course, we have only observed a single reversal in the direction of the RM gradient, and so have no information at this stage about whether this phenomenon is periodic. Therefore, this model remains a possible explanation for the observed RM-gradient reversal, but we currently have no firm evidence in support of this model. If future multifrequency VLBA polarization observations show the presence of periodic reversals of the direction of a transverse RM gradient across the jet, this will provide support for this type of model.

A 'nested-helix' magnetic field structure. Another intriguing possibility is related to magnetic-tower-type scenarios for the launching of jets (Lynden-Bell 1996). In this picture, magnetic field lines anchored in the inner accretion disc are carried outwards along with the jet flow and returned in outer layers of the jet, closing through the outer part of the accretion disc. Combined with the effect of the differential rotation of the accretion disc, this gives rise to a 'nested helical field' structure, with an 'inner' helical field displaying a helicity corresponding to the direction of rotation of the accretion disc and the magnetic polarity of the jet base and an 'outer' helical field displaying the opposite helicity (Fig. 9). The pitch angles of the inner and outer helical fields may be different, most likely with the

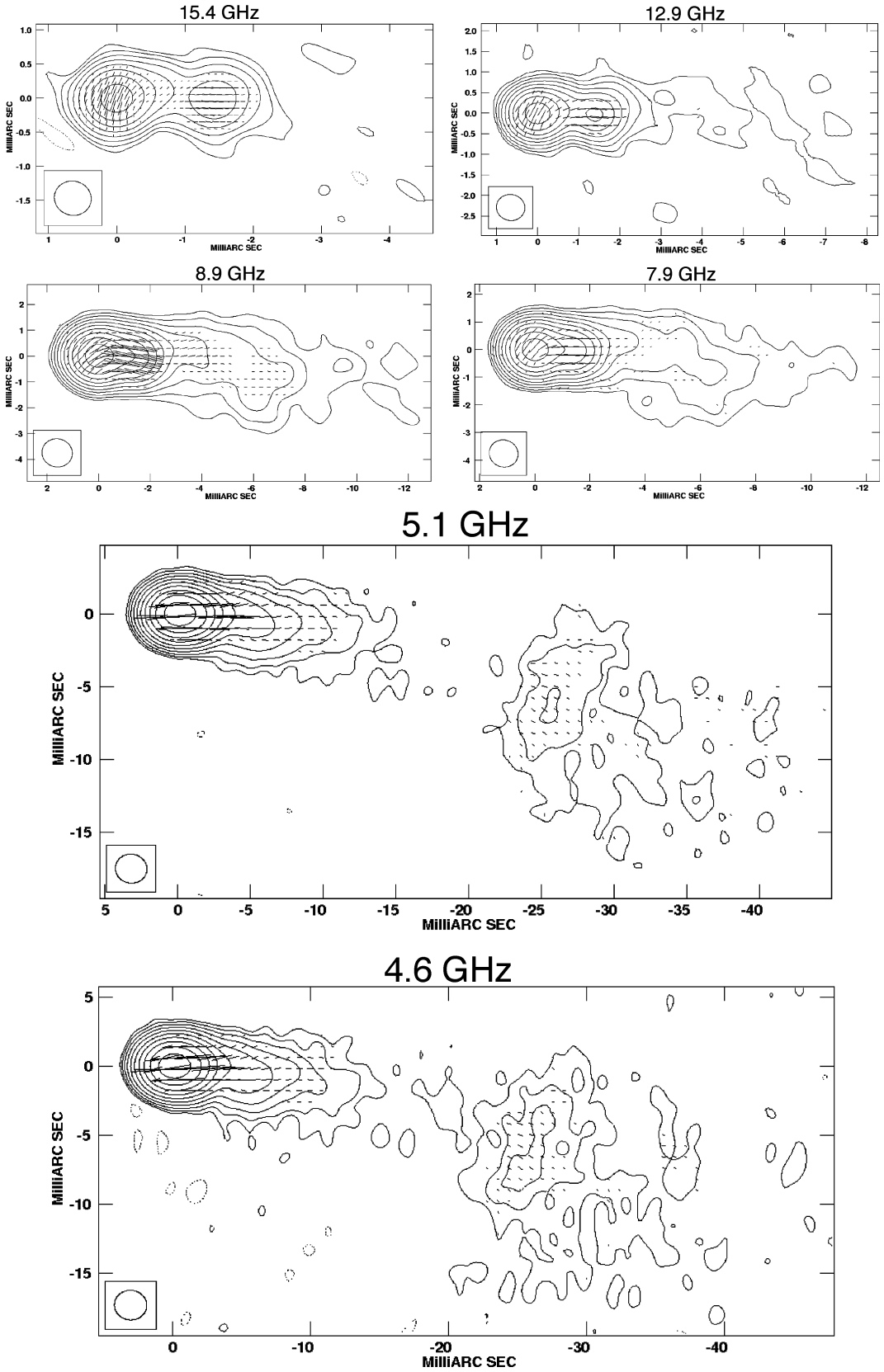


Figure 3. VLBA *I* maps with (electric vector) polarization sticks superimposed at all six frequencies (see Table 1) at epoch 2003 August 22, corrected for integrated Faraday Rotation.

Table 3. Map parameters of Figs 2 and 3.

Epoch	Peak (Jy beam^{-1})†	Bottom contour (mJy beam^{-1})†
2002 August 24	1.7, 1.6, 0.9	0.2, 0.4, 4.5
2003 August 22	1.3, 1.2, 1.3, 1.3, 1.3, 1.2	1.6, 1.5, 1.6, 1.6, 3.3, 5.8

†Listed in the order of ascending frequency (see Table 2).

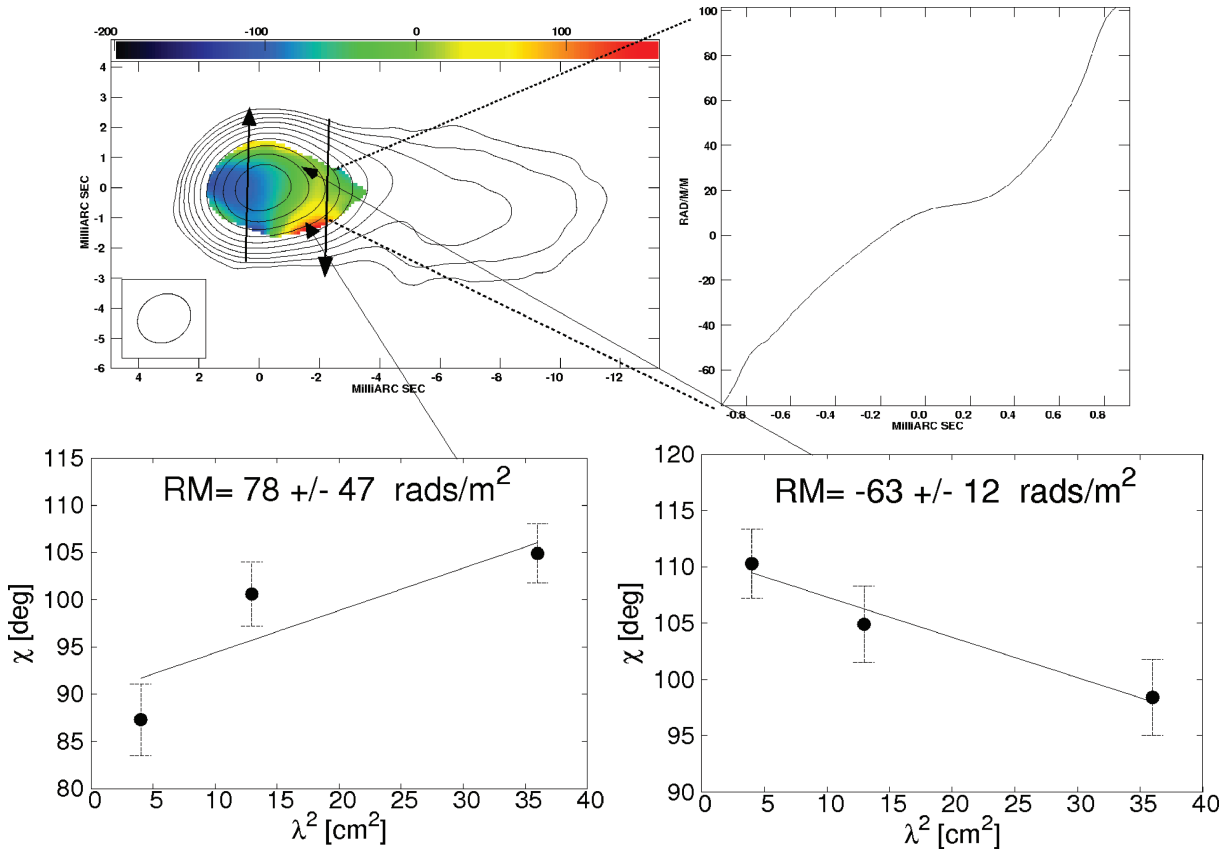


Figure 4. RM map of B1803+784 observed on 1997 April 6. The range of RM values shown in the colour bar is in units of rad m^{-2}. The *I* contours are those for 8.4 GHz. The peak flux (Jy beam^{-1}) is 1.9 Jy beam^{-1} and the lowest contour is 2.0 mJy beam^{-1}. The accompanying panels show a slice of the RM distribution across the jet, and plots of the polarization angle χ versus λ^2 for the indicated 3 × 3 pixel regions near the top and bottom of the jet. The errors shown are 1σ.

inner field having a lower pitch angle (being more tightly wound). The net RM gradient we observe will include contributions from both of these fields, corresponding to the volumes of both of these regions that lie along the line of sight between the emission region and the observer. The directions of the RM gradients associated with each region will be opposite, and the net observed RM gradient will be determined by whether the inner or outer region makes the larger contribution to the net observed RM. In turn, this will be determined by the distribution of the electron density and magnetic field along the jet and with distance from the jet axis. The direction of the observed RM gradient could 'flip' if, for example, the outer region of helical field usually dominates the observed RM distribution, but the inner region of helical field temporarily became dominant due to an increase in the electron density or magnetic field strength in the inner region of helical field. Such variations in electron density and/or magnetic field strength could come about due to variations in activity of the central engine and the ejection of jet material. In this case, the resulting reversals in the direction of the net observed RM gradient would most likely not occur periodically, and may follow activity of the VLBI core. If future observations provide evidence for a connection between epochs when the direction of the transverse RM gradient reverses and periods of enhanced core activity, this will provide support for this type of scenario.

Changes in the distribution of thermal electrons surrounding the jet. Finally, we should consider whether the observed change in the direction of the transverse RM gradient could be due purely to changes in the distribution of thermal gas in the vicinity of the jet, unrelated to the presence of a helical jet magnetic field. Could the transverse gradient in the RM be due, for example, to a gradient in the thermal-electron density across the jet, with the change in the direction of the gradient corresponding to a change in the side of the jet where the electron density was highest? In this scenario, the changes in the observed RM distribution would essentially be due to 'patchiness' in a moving intervening Faraday screen, and so would probably occur fairly randomly with time.

We find this explanation unlikely for several reasons. The first is that our observations and the observations of Zavala & Taylor (2003) consistently show the presence of transverse RM gradients

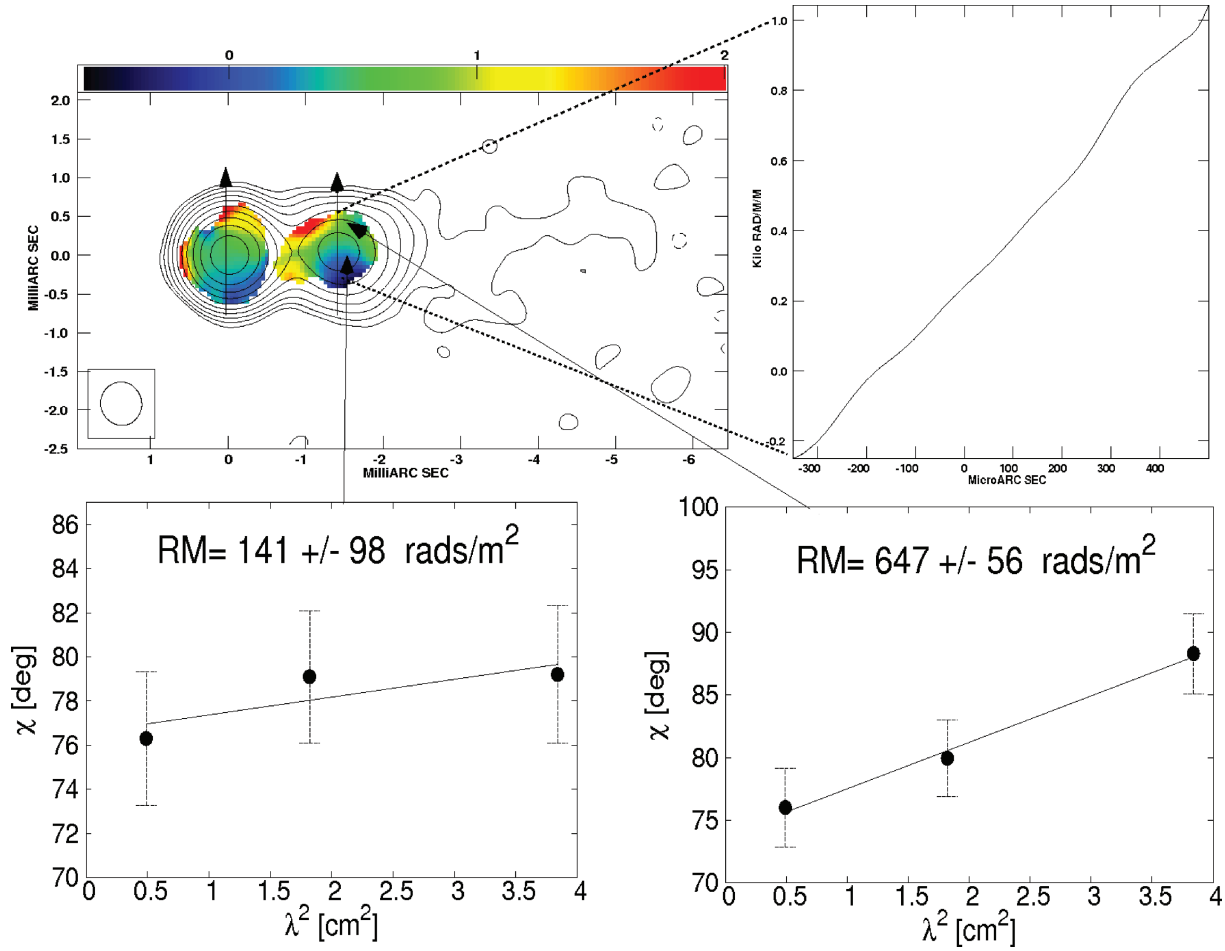


Figure 5. RM map of B1803+784 observed on 2002 August 24. The range of RM values shown in the colour bar is in units of krad m^{-2}. The *I* contours are those for 15.3 GHz. The peak flux is 1.7 Jy $beam^{-1}$ and the lowest contour is 2.0 mJy $beam^{-1}$. The accompanying panels show a slice of the RM distribution across the jet, and plots of polarization angle χ versus λ^2 for the indicated 3 × 3 pixel regions near the top and bottom of the jet. The errors shown are 1σ.

over roughly 6 years, whereas we would expect the RM pattern produced by a moving 'patchy' screen not to be as consistent. Further, in our 1997 RM map (Fig. 4), the RM on the northern side of the jet is negative, whereas the RM on the southern side of the jet is positive: a change of the sign of the RM from one side of the jet to the other is difficult to explain as the result of a patchy thermal-electron distribution, but is quite natural if the observed RM gradient is due to a helical jet magnetic field. With regard to the observed changes in the RM distribution, a comparison of our 1997 and 2003 RM maps (Figs 4 and 6) shows that the RM on the northern side of the jet is negative in 1997, but positive in 2003. Here, also, a change in the thermal-electron distribution is not sufficient to explain these observations: they require that the direction of the line-of-sight component of the magnetic field in the region of Faraday Rotation has changed between these two epochs. Since a change in the line-of-sight magnetic field is required, this makes it natural to consider scenarios involving changes in a helical jet magnetic field structure.

Finally, we note that another possible way to explain time-variable Faraday Rotation is if compact jet components 'illuminate' different regions in a static, inhomogeneous foreground Faraday screen as they move behind it, as was suggested by Zavala & Taylor (2001) for the core RM variations in 3C279. However, this is likewise an unlikely explanation for the RM changes observed for B1803+784, because it is difficult to imagine how this effect could give rise to changes in the RM pattern *across* the jet. In addition, the apparent speeds of VLBI components near the region where we have detected the transverse RM gradients in B1803+784 are low: an essentially quasi-stationary component has been observed roughly 1.5 mas from the core for nearly three decades, and no features detected closer than a few mas from the core show clear motions (Gabuzda & Chernetskii 2003; Kellermann et al. 2004; http://www.physics.purdue.edu/MOJAVE/sepavstime/B1803+784_sepvstime.gif). This likewise appears to make it unlikely that the scenario envisaged for 3C279 is operating in this region of the B1803+784 jet, since none of the observed compact VLBI features displays appreciable motions.

4.2 Propagation of the RM-gradient reversal

It is interesting to consider the possible motion or propagation of the transverse RM-gradient pattern. To compare the distances from the core where the transverse RM gradient is most clearly visible, we must construct RM maps for the different epochs using the same restoring beam. We have used the beam in Fig. 4 for this purpose, and the RM maps for 2002 August and 2003 August constructed using this beam are shown in Fig. 10. We first note that the transverse gradients we initially identified based on the images with their intrinsic beams are still visible in each of these matched-resolution maps. This is particularly important for the 2002 August RM image,

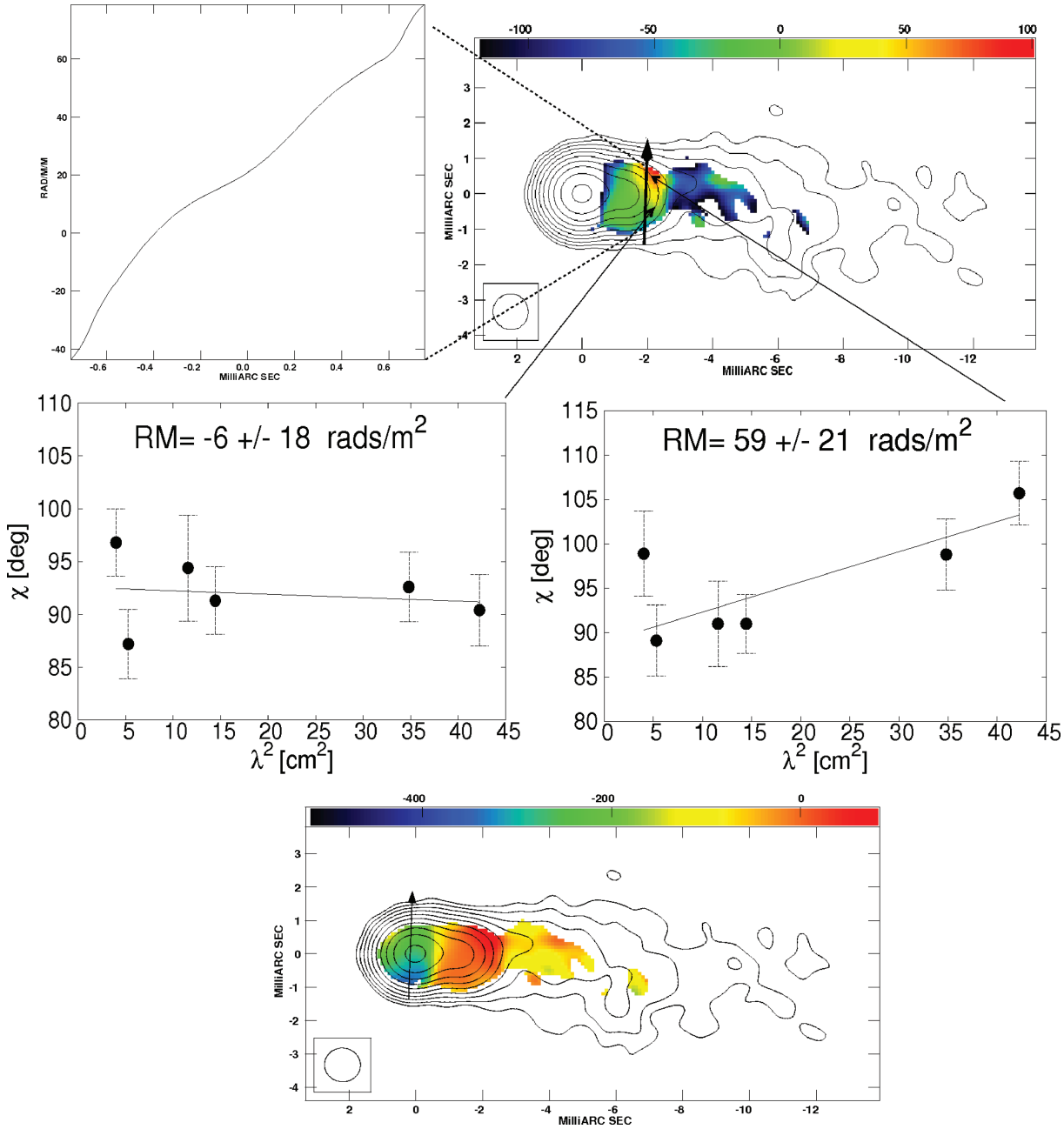


Figure 6. RM maps of B1803+784 observed on 2003 August 22; the two maps correspond to the same RM distribution, but are shown separately with different RM ranges to highlight the RM distributions in the jet (top map) and core (bottom map). The range of RM values shown in the colour bars is in units of rad m^{-2}. The *I* contours are those at 7.9 GHz. The peak flux is 1.2 Jy $beam^{-1}$ and the lowest contour is 2.0 mJy $beam^{-1}$. The accompanying panels show a slice of the RM distribution across the jet, and polarization angle χ versus λ^2 plots for the indicated 3 × 3 pixel regions near the top and bottom of the jet. The errors shown are 1σ.

which was made from data obtained at 15–43 GHz, rather than 5–15 GHz, and so had an intrinsically appreciably higher resolution.

As in Fig. 4, the transverse RM gradient is visible essentially all along the VLBI structure, out to nearly 3 mas from the core. The distances from the core where the transverse RM gradient is most clearly visible in the remaining two matched-resolution images are roughly 1.5–2.0 mas in 1997 April and 2.0–2.5 mas in 2003 August; in the 2000 June RM map of Zavala & Taylor (2003), the RM gradient is most prominent 3–4 mas from the core. (Note that we do not have access to the actual 2000 June RM map of Zavala & Taylor 2003 in electronic form, and so our ability to analyse this image and compare it with the other images considered is quite limited.)

The 1997 April, 2000 June and 2003 August RM maps all have similar intrinsic resolutions, and so the positions where the transverse RM gradients are most clearly visible can be meaningfully compared. However, we see no clear evidence for systematic movement of the observed RM patterns either towards or away from the VLBI core over the time covered by these epochs: the distances from the core are 1.5–2.0 mas in 1997 April, 3–4 mas in 2000 June and 2.0–2.5 mas in 2003 August. This is not entirely surprising, since the separation between our epochs may not be well matched

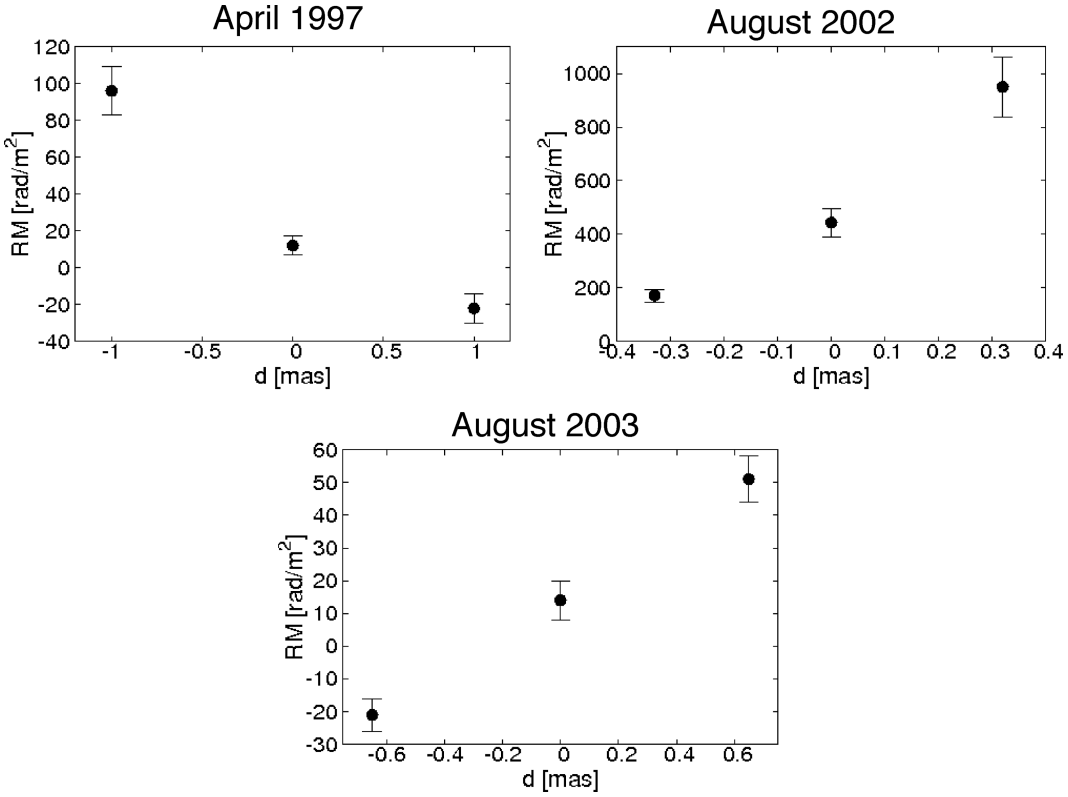


Figure 7. Plots of observed RM as a function of transverse distance d from a reference point $\boldsymbol{P}$ near the central jet spine, for cuts from north to south across the jet and core region of B1803+784 for the three epochs. For 1997 April: $\boldsymbol{P} = (-1.7, -0.1$ mas); for 2002 August: $\boldsymbol{P} = (-1.4, -0.13$ mas) and for 2003 August: $\boldsymbol{P} = (-1.9, -0.05$ mas). The distance d is positive to the north of $\boldsymbol{P}$ and negative to the south of $\boldsymbol{P}$. All errors are 1σ.

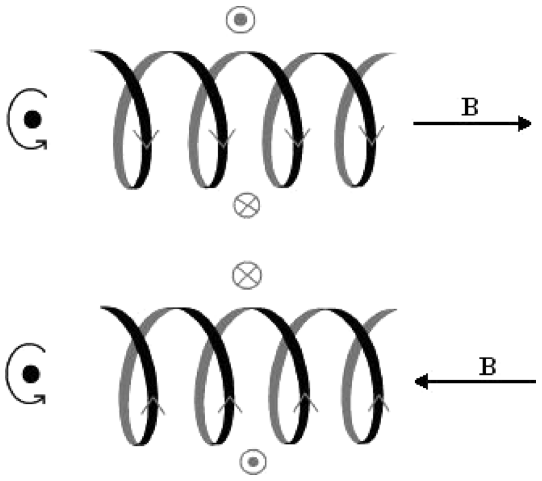


Figure 8. Illustration of how a 'flip' in the RM gradient can be caused by a change in the pole of the black hole facing the Earth. The arrows mark the direction of the $\boldsymbol{B}$ field, and are marked on the nearer side of the helical field to the observer.

to the time-scales on which the RM patterns evolve and/or propagate. For example, if the RM pattern moves with a proper motion of several tenths of a mas per year (typical of superluminal motions in AGN with redshifts similar to B1803+784), it could move and evolve substantially over the 3-year intervals from 1997 April to 2000 June and from 2000 June to 2003 August, making it difficult to track the pattern. At the same time, the general region of the transverse RM gradient is also near the location of a long-lived quasi-stationary feature in the jet of B1803+784, approximately 1.5 mas from the VLBI core (e.g. Gabuzda & Chernetskii 2003; Kellermann et al. 2004). Depending on the origin of this quasi-stationary feature, it may be that RM patterns in this region will also display very low apparent speeds along the jet. More frequent multifrequency monitoring of this AGN with polarization VLBI could provide additional information about the evolution of the RM structure on parsec scales, which could potentially provide firmer constraints on possible models for the origin of the observed RM gradient and its evolution.

5 CONCLUSION

We have detected transverse RM gradients across the VLBI jet of B1803+784 at three different epochs; a transverse RM gradient is also visible in the RM distribution for this AGN published by Zavala & Taylor (2003). The presence of a transverse RM gradient across the jet at four different epochs spanning about 7 years provides firm evidence for a helical $\boldsymbol{B}$ field associated with this jet.

Unexpectedly, a comparison of the RM gradients for these four epochs shows a clear *reversal* of the direction of the gradient between 2000 June and 2002 August. This is not accompanied by any obvious change in the jet intensity or polarization structure.

The origin for this observed 'flip' in the direction of the transverse RM gradient in the jet of B1803+784 is not clear. We have suggested several scenarios that could potentially give rise to this phenomenon: (i) a reversal of the direction of the poloidal component of the intrinsic magnetic field of the central black hole; (ii) a reversal of the direction of the azimuthal field component associated with torsional oscillations of the jet and (iii) a change in whether the

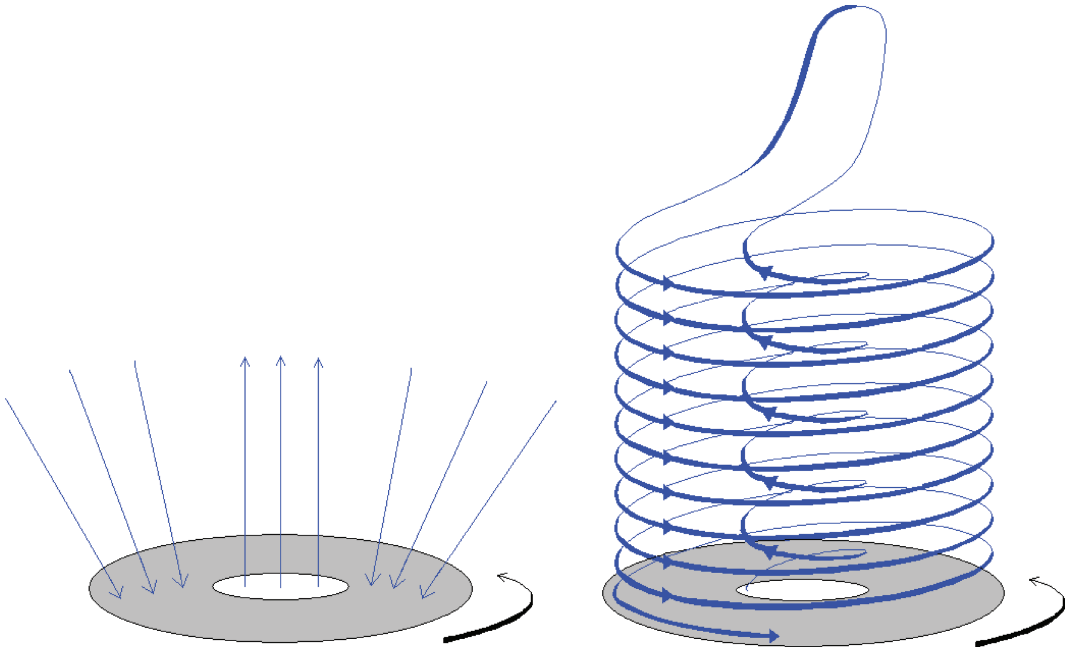


Figure 9. Illustration showing how the magnetic field lines from a magnetic-tower model (with the magnetic field lines going in the direction of outflow, finally looping back down to the accretion disc) can get wound up as an 'inner' and 'outer' helix, as a result of the differential disc rotation. The first figure shows the direction of the magnetic field lines in this model, whereas the second follows the path of one of these magnetic field lines that gets wound up in a 'nested helical field' with the 'inner' helix less tightly wound than the 'outer' helix.

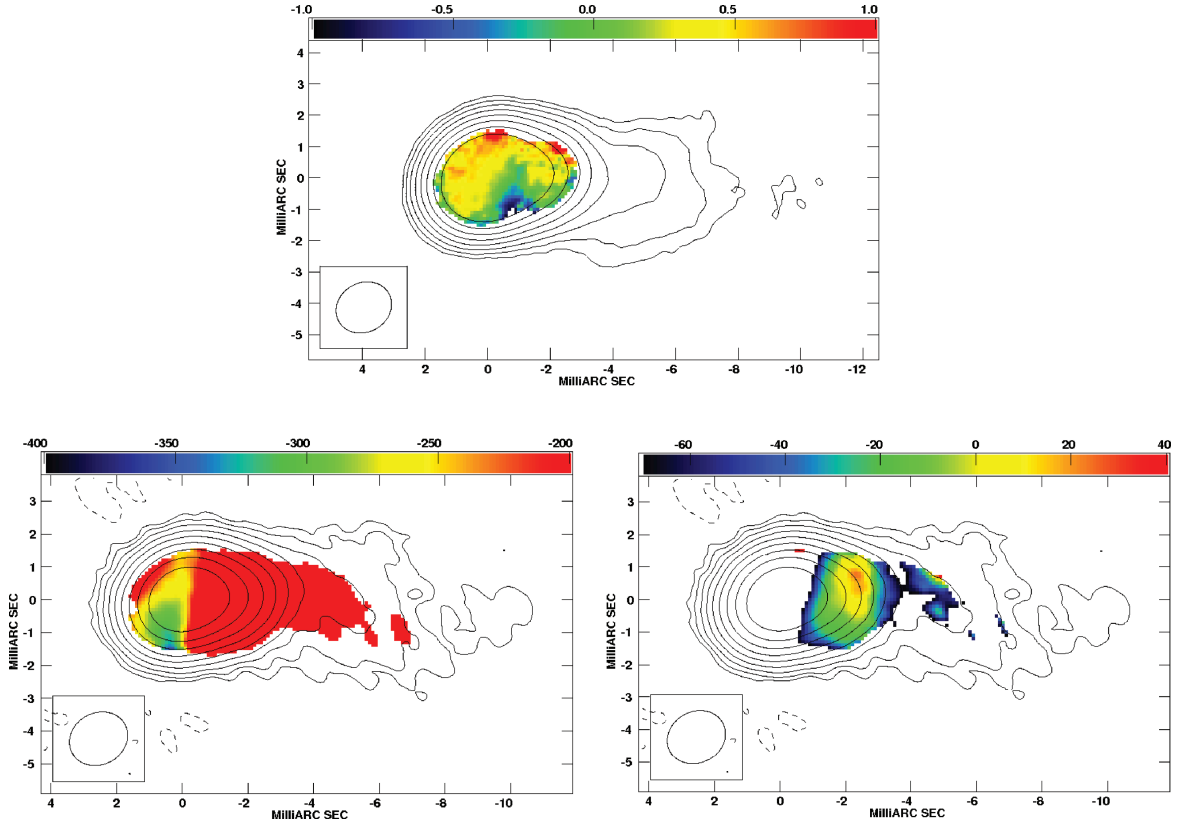


Figure 10. RM maps of B1803+784 observed on 2002 August (top panel) and 2003 August (core region shown in the bottom-left panel and jet in the bottom-right panel), convolved with the same beam as was used for the 1997 April image in Fig. 4. The range of RM values shown in the colour bars for the RM maps is in units of krad m^{-2} (top panel: 2002 August) and in rad m^{-2} (bottom-left and -right panels: 2003 August). The peak fluxes are 1.9 Jy $beam^{-1}$ for 2002 August and 1.4 Jy $beam^{-1}$ for 2003 August; the lowest contours are 2.0 mJy $beam^{-1}$ for both epochs. The transverse gradients identified based on the images with their intrinsic beams are still visible in each of these matched-resolution maps.

'inner' or 'outer' region of helical magnetic field dominates the total observed RM in a magnetic-tower picture. Although it is not possible at this stage to conclusively identify whether any of these scenarios is the origin of the observed RM-gradient reversal, we favour the last hypothesis, because it provides a relatively simple explanation for this seemingly strange event, since a 'nested helix' structure for the jet magnetic field is a natural outcome of magnetic-tower models.

Further multifrequency polarization studies of this source are clearly crucial for our understanding of how the transverse Faraday Rotation gradients evolve over time and with distance from the core. Higher resolution multifrequency VLBI polarization studies can be used to study transverse RM gradients within the observed VLBI core in more detail, as is demonstrated by our 15–43 GHz RM image. We have recently obtained further VLBA polarization observations of B1803+784 at 5–43 GHz, which we hope will enable us to trace the behaviour of the RM distribution over a wider range of distances along the jet, all at a single epoch. Numerical studies to determine the feasibility of various scenarios for the reversal of the transverse RM gradient would also be of considerable interest, and are planned as part of our continuing work in this area.

ACKNOWLEDGMENTS

The research for this publication was financially supported by a Basic Research Grant from Science Foundation Ireland. The National Radio Astronomy Observatory is operated by Associated Universities Inc. We thank P. Cronin for his work on the RM map in 1997 April, Shane O'Sullivan for constructing the helix in Fig. 8, T. V. Cawthorne for useful discussions of these results and the anonymous referee for useful comments and suggestions that have improved this paper.

REFERENCES

Asada K., Inoue M., Uchida Y., Kameno S., Fujisawa K., Iguchi S., Mutoh M., 2002, PASJ, 54, L39
Asada K., Inoue M., Kameno S., Nagai H., 2008a, ApJ, 675, 79
Asada K., Inoue M., Nakamura M., Kameno S., Nagai H., 2008b, ApJ, 682, 798
Bisnovatyi-Kogan G. S., 2007, MNRAS, 376, 457
Burn B. J., 1966, MNRAS, 133, 67
Croke S. M., Gabuzda D. C., 2008, MNRAS, 386, 619
Gabuzda D. C., 1999, New Astron. Rev., 43, 691
Gabuzda D. C., Chernetskii V. A., 2003, MNRAS, 339, 669
Gabuzda D. C., Pushkarev A. B., Cawthorne T. V., 2000, MNRAS, 319, 1109
Gabuzda D. C., Murray É., Cronin P. J., 2004, MNRAS, 351, L89
Gabuzda D. C., Vitrishchak V. M., Mahmud M., O'Sullivan S. P., 2008, MNRAS, 384, 1003
Hallahan R., Gabuzda D. C., 2009, Proc. Workshop on Blazar Variability across the Electromagnetic Spectrum. SISSA, Trieste, p. 40 (http://pos.sissa.it)
Hughes P. A., Aller H. D., Aller M. F., 1989, ApJ, 1, 349, 54
Kellermann K. I. et al., 2004, ApJ, 609, 539
Laing R. A., 1980, MNRAS, 193, 439
Lister M. L., 2001, ApJ, 562, 208
Lovelace R. V. E., Li H., Koldoba A. V., Ustyugova G. V., Romanova M. M., 2002, ApJ, 572, 445
Lynden-Bell D., 1996, MNRAS, 279, L389
Lyutikov M., Pariev V., Gabuzda D. C., 2005, MNRAS, 360, 869
Mahmud M., Gabuzda D. C., 2008, in Travis A. Rector and David S. De Young, eds, ASP Conf. Ser. Vol. 386, Extragalactic Jets: Theory and Observations from Radio to Gamma-rays. Astron. Soc. Pac., San Francisco, p. 494
Nakamura M., Uchida Y., Hirose S., 2001, New Astron., 6, 61
Pacholczyk A. G., 1970, Radio Astrophysics. Freeman & Co., San Francisco
Pushkarev A. B., 2001, Astron. Rep., 45, 667
Reynolds C., Cawthorne T. V., Gabuzda D. C., 2001, MNRAS, 327, 1071
Zavala R. T., Taylor G. B., 2001, ApJ, 550, L147
Zavala R. T., Taylor G. B., 2003, ApJ, 589, 126
Zavala R. T., Taylor G. B., 2005, ApJ, 625, L73

APPENDIX A

To illustrate why the presence of a RM gradient will not be affected by incorrect EVPA calibration, we consider first the definition of the RM, measured by comparing the polarization angles χ_1 and χ_2 measured at two wavelengths λ_1 and λ_2:

$$\mathrm{RM} = \frac{\mathrm{d}\chi}{\mathrm{d}\lambda^2} = \frac{\chi_2 - \chi_1}{\lambda_2^2 - \lambda_1^2}. \quad \text{(A1)}$$

The RM gradient between two points a and b is essentially the difference in the RM values measured at these two points:

$$\mathrm{RM}(a) - \mathrm{RM}(b) = \frac{\chi_2(a) - \chi_1(a)}{\lambda_2^2 - \lambda_1^2} - \frac{\chi_2(b) - \chi_1(b)}{\lambda_2^2 - \lambda_1^2} \quad \text{(A2)}$$

$$= \frac{\chi_2(a) - \chi_2(b)}{\lambda_2^2 - \lambda_1^2} - \frac{\chi_1(a) - \chi_1(b)}{\lambda_2^2 - \lambda_1^2}. \quad \text{(A3)}$$

We can see through the simple rearrangement in the second equation above that, although uncertainty in the absolute EVPA calibration will contribute to the absolute uncertainties of the RM values, the effects of incorrect EVPA calibration essentially cancel out when calculating the RM *gradient*, since they will appear in the same way in the polarization angles measured at each point in the image at the wavelength in question, for example in $\chi_2(b)$ and $\chi_2(a)$. This fact must be taken into account when comparing RM values at different points in an image and their uncertainties in order to estimate the significance of observed RM gradients. For this reason, we have estimated the uncertainties in the RM values at a given location in the map in Fig. 7 purely from the rms deviation of the RM values in a 3×3 pixel area surrounding this location, rather than using the formal uncertainties from the fits yielding the RM values, since the latter will be affected by possible inaccuracies in the EVPA calibrations.

This paper has been typeset from a TEX/LATEX file prepared by the author.